Optical and Acoustical Methods in Science and Technology

Upconversion Luminescence in Yb^{3+}/Tm^{3+} Doped Double Clad Optical Fibre

J. Zmojda, D. Dorosz*, M. Kochanowicz and J. Dorosz

Department of Optoelectronics and Lighting Technology, Białystok University of Technology

Wiejska 45, 15-351 Białystok, Poland

The paper presents luminescence properties of telluride glass doped with Yb^{3+}/Tm^{3+} ions. Strong blue emission at 477 nm corresponding to the transition ${}^1G_4 \rightarrow {}^3H_6$ in thulium ions was measured under the excitation of a 976 nm diode laser. The dependence of the upconversion emission upon the thulium ions concentration was studied in order to determine the optimal ion content. The results showed that intensity of upconversion emission enhances, with the increase of Tm^{3+} content up to 0.1 mol.%. The most effective energy transfer $Yb^{3+} \rightarrow Tm^{3+}$ occurs in the glassy matrix with molar ratio of dopant 1 Yb^{3+} : 0.1 Tm^{3+}. Double-clad optical fibre was made of glass with the highest upconversion intensity at the wavelength of $\lambda = 477$ nm (TGPF101). As a result of optical excitation ($\lambda = 976$ nm) of the produced optical fibre, an additional emission line, which was not noticed in the glass, was observed at the wavelength of 351 nm corresponding to the ${}^1D_2 \rightarrow {}^3H_6$ transition.

PACS: 42.81.−i, 42.79.Ag, 33.20.Kf, 42.25.Bs

1. Introduction

The needs of contemporary optoelectronics impose the search for new glassy materials that are able to propagate electromagnetic radiation over a broad spectrum range. The choice of matrix and optimization of its chemical, electrooptical and magnetooptical properties determine the range of their applications [1–3]. Low phonon energy in telluride glasses (≈ 750 cm^{-1}) has an impact on the reduced effect of multiphonon relaxation, thus preventing high radiant emission to be obtained. Therefore, telluride glasses are usually applied in optical waveguides [2–6]. Solid-body lasers emitting radiation within the blue wavelength range are commonly used nowadays in data recording/reading systems in HD quality, colour displays or diagnostic medicine. Obtaining efficient blue upconversion in glass matrices applied on the core of fibre lasers is possible thanks to the use of a rare earth element, such as thulium [7]. The increase in the luminescence band intensity resulting from transitions in the structure of thulium energy levels is attainable due to introduction of a sensitizer in the form of Yb^{3+} ions [7].

In this article a series of telluride glasses doped with the Yb^{3+}/Tm^{3+} ion system was presented in order to determine the conditions of energy transfer between energy levels of active dopants. The analysis of population density at the levels of metastable dopants was carried out. The determined luminescence parameters suggest the possibility of applying the produced glasses in fibre lasers generating radiation in the visible spectrum. In this article tellurium glass doped with Yb^{3+}/Tm^{3+} ions is presented. As a result of exciting with a laser diode ($\lambda = 976$ nm) the effect of luminescence at the wavelength of 477 nm (${}^1G_4 \rightarrow {}^3H_6$) was observed, which appeared due to upconversion in the energy structure in Tm^{3+} ions.

2. Experiment

The TeO_2–GeO_2–PbO–PbF_2–BaO–Nb_2O_5–LaF_3 system glasses doped with Yb^{3+}/Tm^{3+} ions were melted from spectrally pure (99.99%) raw materials. The homogenized set was placed in a platinum crucible and melted in an electric furnace in temperature of 900 °C for 30 min in an argon atmosphere. The molten glass was poured out onto a brass plate and then exposed to the process of annealing in the temperature approximate to the transformation temperature for 12 h. Homogeneous and transparent glasses were obtained without visible effect of crystallization. In order to determine spectral properties a series of samples with the dimensions of $8 \times 8 \times 3$ mm^3 were prepared. The spectral transmission measurement within the range from 0.5 to 1.7 μm was taken using an Acton Spectra Pro 2300i monochromator with an InGaAs detector, and within the range from 2.5 to 50 μm with a SPECORD M80 spectrophotometer. The glass density, ρ, was calculated using the method of hydrostatic weighing. The refractive index (633 nm) was determined with the aid of a Metricon 2010 refractometer. The characteristic temperatures of the obtained glasses were calculated based on the measurement taken with a SETARAM Labsys thermal analyzer using the differential scanning calorimetry (DSC) method. The luminescence spectrum within the range from 400 to 700 nm was measured at a station equipped with a Hamamatsu TM-C10082CAH spectrometer and a laser diode ($\lambda_p = 976$ nm) with an optical fibre output having the maximum optical power $P = 30$ W.

* corresponding author; e-mail: domdor@pb.edu.pl

3. Results and discussion

In Table I the parameters of tellurium-based oxide-fluoride glasses doped with Yb^{3+} and Tm^{3+} are presented. The produced glasses because of the prevailing concentration of Te^{4+} ions have optical properties similar to well-known telluride glasses.

TABLE I

Optical and physical properties of telluride glass.

Parameter	Value
refractive index n (633 nm)	2.074
mass density ρ [g/cm^3]	6.21
transmission [μm]	0.3–5.5
thermal expansion coefficient α_{100}^{400} [10^{-7} 1/K]	108.9
dilatometric softening point T_s [°C]	364
transformation temperature [°C] (DSC)	345

The light transmission in the visual and the near infrared spectrum is at the level of 90%, which has a considerable impact on the pumping efficiency and energy transfer between active dopants. Moreover, the main advantage of the produced glasses is their high thermal stability determined on the basis of DSC measurement. The lack of exothermic peak (DSC) indicating glass crystallization was confirmed through experimentation and transmission losses resulting from multiple remelting of the glass were not found.

3.1. Absorption coefficient

Based on spectral transmission the absorption coefficient spectrum of the obtained glass doped with Yb^{3+} and Tm^{3+} ions (Fig. 1) was calculated. Absorption bands originating from the complex structure of thulium corresponding to the following transitions: $^3H_6 \rightarrow {}^3F_4$, $^3H_5$, $^3H_4$, $^3F_2 + {}^3F_3$ were observed, as well as the band characteristic of the ion of ytterbium, corresponding to the $^2F_{7/2} \rightarrow {}^2F_{5/2}$ transition. Transitions from the ground state to higher energy levels were described by the Paschen notation [7]. The high concentration of ytterbium in the matrix results in strong radiation absorption at the wavelength of 978 nm, thus facilitating efficient excitation of the Yb^{3+}/Tm^{3+} system.

In practice, because of the excitation bandwidth and high quantum efficiency ($\approx 90\%$), Yb^{3+} ions are used as sensitizers in upconversion systems [5, 7].

3.2. Glass luminescence and analysis of the influence of Tm^{3+} concentration on the efficiency of energy transfer

As a result of exciting glasses with the 976 nm wavelength radiation, two anti-Stokes luminescence lines were obtained, the first one was located at 477 nm, corresponding to the $^1G_4 \rightarrow {}^3H_6$ quantum transition, and the second at 651 nm, corresponding to the $^1G_4 \rightarrow {}^3F_4$ transition (Fig. 2). The relation between the upconversion

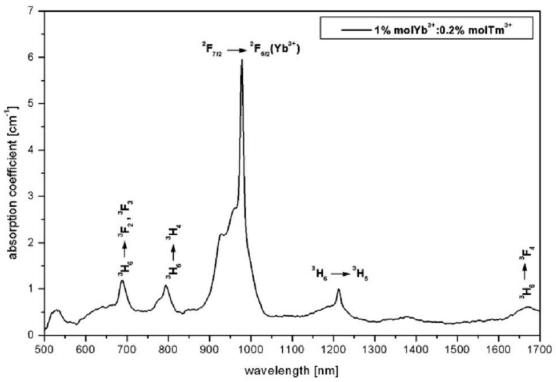

Fig. 1. Absorption coefficient of glass TGPF051.

emission intensity I_{UP} from the pump intensity I_{IR} is determined by the condition:

$$I_{UP} \propto I_{IR}^n \,, \tag{1}$$

where n is the number of photons absorbed in the infrared to the number of photons emitted in the visual spectrum. The rise in the pump radiation intensity increases the number of absorbed photons to the Yb^{3+} laser level, and according to condition (1), the emission intensity in the visual spectrum increases [5].

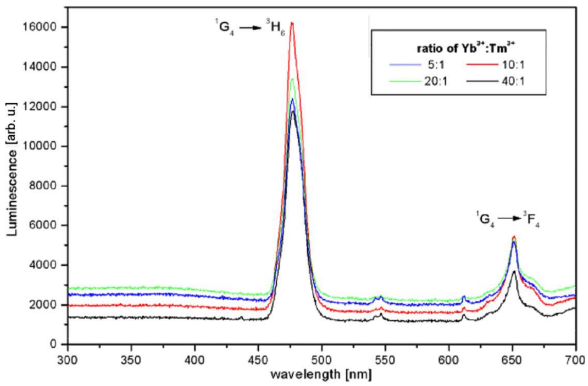

Fig. 2. Comparison of spectral luminescensce for different Yb^{3+}/Tm^{3+} ions ratio.

In order to increase the number of ions taking part in the process of upconversion, the constant excitation power was maintained with the variable concentration of Tm^{3+} ions. On the basis of the Dexter model, the probability of nonradiative energy transfer (W_{DA}) is determined by the formula [8]:

$$W_{DA}(R) = \frac{C_{DA}}{R^6} \,, \tag{2}$$

where C_{DA} — micro-parameter of the energy transfer between the donor and the acceptor, $R = ((3/4\pi)N)^{1/3}$ determines the mean distance between the active centres of ytterbium and thulium ions, N — total concentration of Yb^{3+} and Tm^{3+} ions in a given matrix (Table II).

TABLE II

Total concentration of dopants N and average intraionic distance R.

Glass	Yb_2O_3 [mol.%]	Tm_2O_3 [mol.%]	N [10^{20} ions/cm^3]	R [Å]
TGPF051	1	0.2	5.16	7.73
TGPF101	1	0.1	4.74	7.95
TGPF201	1	0.05	4.52	8.08
TGPF401	1	0.025	4.42	8.14

The greater the number of thulium ions is, the smaller is the distance between the centres of active dopants, thus the probability of the $Yb^{3+} \rightarrow Tm^{3+}$ energy transfer is higher. In Fig. 3 the change of the emission intensity into 477 nm and 651 nm in the function of Tm_2O_3 molar content is presented. It should be noted, however, that as the number of thulium ions was higher, the most efficient energy transfer was obtained in the glass doped with RE ions in the following proportion: 1.0 mol.% Yb^{3+} : 0.1 mol.% Tm^{3+}. In other cases the upconversion intensity is lower.

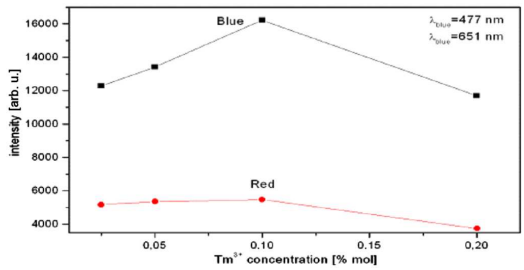

Fig. 3. Upconversion intensity of transitions at 477 nm ($^1G_4 \rightarrow {}^3H_6$) and 651 nm ($^1G_4 \rightarrow {}^3F_4$) in function of molar concentration Tm_2O_3 ions.

For low concentrations of the Tm^{3+} ion the mean atomic distance (R) is big enough to enable energy transfer with a smaller number of active centres. On the other hand, the increase in thulium ion concentration over 0.1 mol.% results in the effect of reverse energy transfer from $Tm^{3+} \rightarrow Yb^{3+}$, which leads to a rapid quenching of the luminescence line at the wavelength 477 nm [9].

3.3. Optical fibre luminescence

As a result of analysing thermal and optical properties of telluride glasses a double-clad optical fibre was produced. The core was made of the glass with the highest emission intensity of the $^1G_4 \rightarrow {}^3H_6$ transition (TGPF101). Figure 4a shows the cross-section of the optical fibre with a core made of telluride glass doped with Yb^{3+}/Tm^{3+} ions. A high value of numerical aperture NA ≈ 1 ($\lambda = 633$ nm) permits easy coupling of the pump with the fibre and efficient excitation of the active core (Fig. 4b).

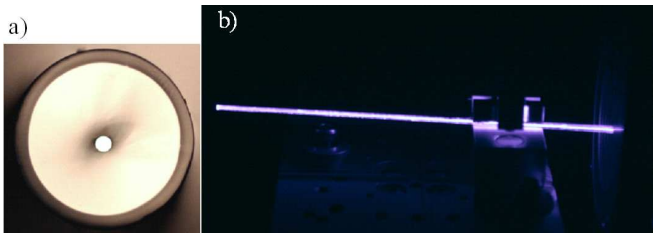

Fig. 4. Cross-section of optical fibre ($d_{\text{core}} = 40$ μm, $D_{\text{fibre}} = 450$ μm) (a) and photograph of blue emission in double-clad fibre ($l = 10$ cm) excited at 976 nm (b).

Figure 5 shows the luminescence spectrum obtained as a result of exciting the optical fibre with the 976 nm wavelength pump radiation. The pump power, introduced directly into the optical fibre face, amounted to $P_{\text{opt}} = 2$ W. While compared to the glass luminescence spectrum, in the optical fibre an additional emission line was observed at the wavelength of 351 nm, corresponding to the $^1D_2 \rightarrow {}^3H_6$ transition.

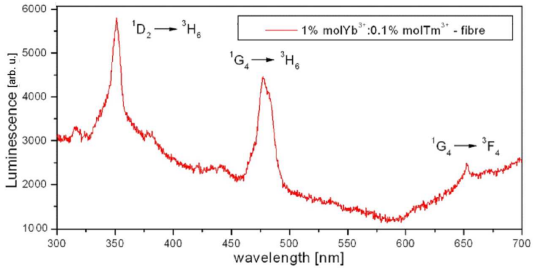

Fig. 5. Luminescence spectra of optical fibre doped with 1 mol.%Yb^{3+} : 0.1 mol.%Tm^{3+}.

Such an effect usually appears in fluoride glasses [10] and in case of the produced optical fibre it is the result of using fluoride compounds, such as PbF_2 and LaF_3. In addition, because of the high numerical aperture, large power densities of the pump radiation in the fibre were obtained, which leads to the effect of phonon summation by energy transfer in the energy structure of the Tm^{3+} ion [11].

3.4. Mechanism of upconversion

The mechanism of upconversion appearing in the Yb^{3+}/Tm^{3+} ion system excited with the 976 nm wavelength radiation is related to quantum effects occurring between active dopant centres [12]. Because of the discrepancy between the energy levels of Tm^{3+} and Yb^{3+} ions, the interdipole interaction has a non-resonant character and the energy transfer is nonradiative with the participation of phonons [13]. The process of excitation conversion is shown schematically in Fig. 6, in which dashed lines indicate transfers of an energy quantum from three successive relaxing photons from the excited level of the Yb^{3+} ion. The population of the $^1G_4$ level, while being excited with the pump radiation (978 nm), has been described in the following steps [12, 14]:

I. The Yb^{3+} ion transiting from the excited state some part of energy to Tm^{3+} ions, thus leading to population of the $^3H_5$ level. A short lifetime and a small difference in energy lead to a rapid nonradiative relaxation to the $^3F_4$ level.

$$\mathrm{Yb}(^2F_{5/2}) + \mathrm{Tm}(^3H_6) \rightarrow \mathrm{Yb}(^2F_{7/2}) + \mathrm{Tm}(^3H_5) \rightarrow \mathrm{Yb}(^2F_{7/2}) + \mathrm{Tm}(^3F_4)\,. \quad (3)$$

II. At that time the successive Yb^{3+} ion transferring an energy quantum in a nonradiative way generates excitation of the Tm^{3+} ion to the $^3F_2$ level. Similarly to case (3), as a result of a rapid multiphonon relaxation, the population of the $^3H_4$ lower excited level takes place

$$\mathrm{Yb}(^2F_{5/2}) + \mathrm{Tm}(^3F_4) \rightarrow \mathrm{Yb}(^2F_{7/2}) + \mathrm{Tm}(^3F_2) \rightarrow \mathrm{Yb}(^2F_{7/2}) + \mathrm{Tm}(^3H_4)\,. \quad (4)$$

III. Analogically, the absorption from the $^3H_4$ excited state occurs in consequence of the energy transfer from the third in turn Yb^{3+} ion, leading to population of the $^1G_4$ level

$$\mathrm{Yb}(^2F_{5/2}) + \mathrm{Tm}(^3H_4) \rightarrow \mathrm{Yb}(^2F_{7/2}) + \mathrm{Tm}(^1G_4)\,. \quad (5)$$

As a result of the three-photon process of excitation conversion a strong emission at the wavelength of 477 nm ($^1G_4 \rightarrow {}^3H_6$) was obtained. Simultaneously, a weaker luminescence line appears at the wavelength of 651 nm corresponding to the $^1G_4 \rightarrow {}^3F_4$ transition.

IV. The ultraviolet emission observed in the luminescence spectrum of the optical fibre occurred as a result of cross relaxation between thulium ions in the excited state [12]:

$$\mathrm{Tm}(^3F_2) + \mathrm{Tm}(^3H_4) \rightarrow \mathrm{Tm}(^3H_6) + \mathrm{Tm}(^1D_2)\,. \quad (6)$$

In consequence of the interaction the Tm^{3+} ion transiting from the $^3F_2 \rightarrow {}^3H_6$ level transfers some energy to the ions on the $^3H_4$ level, inducing absorption and population of the $^1D_2$ level. The luminescence line at the wavelength of 351 nm appeared as a result of the $^1D_2 \rightarrow {}^3H_6$ transition.

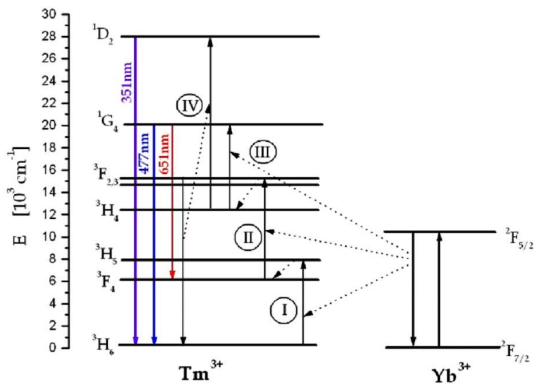

Fig. 6. Simplified diagram of energy level Yb^{3+}/Tm^{3+} with energy transfer mechanism.

3.5. Population density kinetics on metastable levels

Based on the mathematical model of energy transfer in the Yb^{3+}/Tm^{3+} ion system presented in the article [15] a numerical analysis of population densities on metastable levels was carried out. A glass with the highest luminescence level (TGPF101) was used for calculations, disregarding the influence of the $Tm^{3+} \rightarrow Yb^{3+}$ energy transfer [16]. Additionally, because of a rapid multiphonon relaxation ($\approx 10^7$ s^{-1}) leading to a strong population of the $^3F_4$ and $^3H_4$ metastable levels, the zero population of the $^3H_5$ and $^3F_2(^3F_3)$ levels was assumed [17]:

$$\frac{\mathrm{d}N_{\mathrm{Yb1}}}{\mathrm{d}t} = R_{01}N_{\mathrm{Yb0}} - C_{\mathrm{DA2}}N_{\mathrm{Yb1}}N_{\mathrm{Tm0}} - C_{\mathrm{DA4}}N_{\mathrm{Yb1}}N_{\mathrm{Tm1}} - C_{\mathrm{DA6}}N_{\mathrm{Yb1}}N_{\mathrm{Tm3}} - \frac{N_{\mathrm{Yb1}}}{\tau_{\mathrm{Yb1}}}\,, \quad (7)$$

$$\frac{\mathrm{d}N_{\mathrm{Tm1}}}{\mathrm{d}t} = C_{\mathrm{DA2}}N_{\mathrm{Yb1}}N_{\mathrm{Tm0}} - C_{\mathrm{DA4}}N_{\mathrm{Yb1}}N_{\mathrm{Tm1}} + (A_{32}+A_{31})N_{\mathrm{Tm3}} + (A_{62}+A_{61})N_{\mathrm{Tm3}} - \frac{N_{\mathrm{Tm1}}}{\tau_{\mathrm{Tm1}}}\,, \quad (8)$$

$$\frac{\mathrm{d}N_{\mathrm{Tm3}}}{\mathrm{d}t} = C_{\mathrm{DA4}}N_{\mathrm{Yb1}}N_{\mathrm{Tm1}} - C_{\mathrm{DA6}}N_{\mathrm{Yb1}}N_{\mathrm{Tm3}} + (A_{65}+A_{64}+A_{63})N_{\mathrm{Tm6}} - \frac{N_{\mathrm{Tm3}}}{\tau_{\mathrm{Tm3}}}\,, \quad (9)$$

$$\frac{\mathrm{d}N_{\mathrm{Tm6}}}{\mathrm{d}t} = C_{\mathrm{DA6}}N_{\mathrm{Yb1}}N_{\mathrm{Tm3}} - \frac{N_{\mathrm{Tm6}}}{\tau_{\mathrm{Tm6}}}, \quad (10)$$

where R_{01} — the pumping speed of Yb^{3+} ions, $N_{\mathrm{Yb0}}, N_{\mathrm{Tm0}}$ — population densities on the ground level for ytterbium and thulium, respectively. The lifetimes of the upper laser levels of the τ_{Yb} and τ_{Tm} dopants and probabilities of radiative transitions of the A_j acceptor were determined on the basis of the publications [17–21], assuming the lack of interaction between active dopant centres. The energy transfer coefficients $C_{\mathrm{DA}i} = W_{\mathrm{DA}}R^6$ between the excited ion of the donor and the i-th level of the acceptor ion were calculated on the basis of the Miyakawa–Dexter model [22]:

$$W_{\mathrm{DA}} = \frac{2\pi}{\hbar}|H_{\mathrm{DA}}|^2 S_{\mathrm{DA}}\,, \quad (11)$$

where H_{DA} is the Hamiltonian operator of interaction, S_{DA} — spatial overlap of active cross-sections between the acceptor absorption and the donor emission. The pumping speed was determined according to the relation $R_{01} = P\sigma_{\mathrm{abs}}/Ah\nu$, where P is the pump optical power, A — cross-section of the pumping radiation beam, σ_{abs} — active cross-section to the absorption for the pump wavelength, $h\nu$ — the pump photon energy.

In order to solve the system of differential Eqs. (7)–(10) the Runge–Kutta method was used, assuming the zero population of energy levels at the moment $t = 0$. The parameters used in the presented kinetic model of population densities on metastable levels are specified in Table III.

TABLE III

Parameters used in numerical analysis of population densities.

Parameter	Value	Parameter	Value	Parameter	Value
P	200 mW/1000 mW	σ_{abs}	1.45×10^{-20} cm^2	A	0.1 mm^2
ν	3.06×10^{14} s^{-1}	h	6.63×10^{-34} J/s	N_{Tm}	4.36×10^{19} ion/cm^3
N_{Yb}	4.31×10^{20} ion/cm^3	A_{31}	198 s^{-1}	A_{31}	66 s^{-1}
A_{61}	274 s^{-1}	A_{62}	1038 s^{-1}	A_{63}	410 s^{-1}
A_{64}	93 s^{-1}	A_{65}	39 s^{-1}	τ_{Tm1}	705 μs
τ_{Tm3}	223 μs	τ_{Tm6}	386 μs	τ_{Yb1}	989 μs
C_{DA2}	1.41×10^{-17}	C_{DA4}	1.27×10^{-17}	C_{DA6}	1.67×10^{-17}

Figure 7 shows the results of the analysis carried out on the population density kinetics on the $^3H_4$, $^3F_4$ and $^1G_4$ levels of the Tm^{3+} ion and the $^2F_{5/2}$ level of the Yb^{3+} ion. The rise in the pump power results in the simultaneous increase in the number of ytterbium ions taking part in the process of energy transfer. For $P_{\mathrm{pomp}} = 1$ W all ytterbium ions become excited to the $^2F_{5/2}$ level, from which, in consequence of the $^2F_{5/2} \rightarrow {}^2F_{7/2}$ transition, a nonradiative transfer of energy to thulium occurs, leading to the increase in population densities of its higher energy states (Fig. 7b).

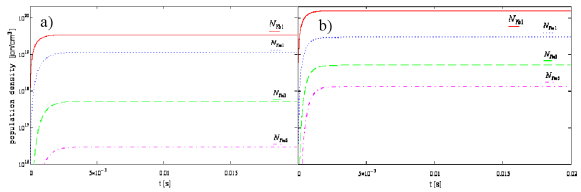

Fig. 7. Population density in time for two pump power: 200 mW (a) and 1000 mW (b).

Analysing the results of the presented model it should be noted that the rise in the pump power increases both the density and the speed of populations in the energy structure of Tm^{3+}, which results in the growth of the emission intensity from the $^1G_4$ into the $^3H_6$ level ($\lambda =$ 477 nm).

4. Conclusions

As a result of the conducted research a thermally stable telluride glass doped with the Yb^{3+}/Tm^{3+} ion system was obtained. The produced glass is characterised by low-energy lattice vibrations, and the introduction of fluoride compounds, such as PbF_2 and LaF_3, enabled to use a high concentration of rare earth elements (1.2 mol.%). While exciting obtained glasses with a 976 nm wavelength laser diode, a strong blue emission corresponding to the $^1G_4 \rightarrow {}^3H_6$ transition in the energy structure of Tm^{3+} ions was observed. Analysing the influence of the content of Tm^{3+} ions on the level of luminescence obtained by the mechanism of upconversion it was established that the most effective energy transfer between $Yb^{3+} \rightarrow Tm^{3+}$ ions took place in the matrix doped in the following proportion: 1 Yb^{3+} : 0.1 Tm^{3+} (mol.%). Based on the non-resonant process of energy transfer between Yb^{3+} and Tm^{3+} ions the mechanism of upconversion was discussed. The energy transfer coefficients, W_{DA}, were calculated using the Miyakawa–Dexter model. The description of the upconversion mechanism was suggested based on the mathematical model of the population density kinetics on metastable levels of the Tm^{3+} ion. For the pump power $P_{\mathrm{pomp}} = 1$ W all ytterbium ions become excited to the $^2F_{5/2}$ level, from which, in consequence of the $^2F_{5/2} \rightarrow {}^2F_{7/2}$ transition, a nonradiative transfer of energy to thulium occurs, leading to the increase in population densities of its higher energy states. As a result of analysing thermal and optical properties of telluride glasses, a double-clad optical fibre was produced using the double crucible method. The core was made of a glass with the highest upconversion intensity at the wavelength of $\lambda = 477$ nm (TGPF101). As a result of optical excitation ($\lambda = 976$ nm) of the produced optical fibre, an additional emission line, which was not noticed in the glass, was observed at the wavelength of 351 nm corresponding to the $^1D_2 \rightarrow {}^3H_6$ transition. Such an effect usually appears in fluoride glasses [12], and in case of the obtained fibre results from using fluoride compounds, such as PbF_2 and LaF_3.

Acknowledgments

This work was supported by Ministry of Science and High Education of Poland — grant No. N N515 512340.

References

[1] B. Richards, S. Shen, A. Jha, Y. Tsang, D. Binks, *Opt. Expr.* **15**, 11 (2007).

[2] B. Pustelny, T. Pustelny, *Acta Phys. Pol. A* **116**, 383 (2009).

[3] T. Pustelny, C. Tyszkiewicz, K. Barczak, *Opt. Appl.* **32**, 469 (2003).

[4] J.S. Wang, E.M. Vogel, E. Snitzer, *Opt. Mater.* **3**, 187 (1994).

[5] L. Feng, Q. Tang, L. Liang, J. Wang, H. Liang, Q. Su, *J. Alloys Comp.* **16**, 436 (2007).

[6] T. Pustelny, K. Barczak, K. Gut, J. Wojcik, *Opt. Appl.* **34**, 531 (2004).

[7] M. Digonet, *Rare-Earth-Doped Fiber Lasers and Amplifiers*, CRC Press Publishers, England, 2001, Ch. 3.

[8] U.R. Rodriguez-Mendoza, V.D. Rodriguez, L.R. Martin, V. Latin, J. Mendez-Ramos, P. Nunez, *J. Alloys Comp.* **32**, 759 (2001).

[9] G. Wang, S. Dai, J. Zhang, J. Yang, Z. Jiang, *J. Mater. Sci.* **23**, 3498 (2007).

[10] N. Rakov, G. Maciel, M. Sundheimer, L. Menezes, A. Gomes, Y. Messaddeq, F. Cassanjes, G. Poirier, S. Ribeiro, *J. Appl. Phys. Commun.* **92**, 6337 (2002).

[11] R. Scheps, *Prog. Quant. Electron.* **20**, 271 (1996).

[12] G. Qin, W. Qin, Ch. Wu, S. Huang, D. Zhao, J. Zhang, S. Lu, *Opt. Commun.* **242**, 346 (2004).

[13] Q. Nie, X. Li, S. Dai, X.S. Wang, X. Shen, *J. Lumin.* **128**, 883 (2008).

[14] H. Lin, K. Liu, L. Lin, Y. Hou, D. Yang, T. Ma, E.Y.B. Pun, *Spectrochim. Acta Part A* **65**, 1035 (2006).

[15] B. Peng, T. Izumitani, *Opt. Mater.* **4**, 701 (1995).

[16] G. Wang, S. Dai, J. Zhang, J. Yang, Z. Jiang, *J. Mater. Sci.* **20**, 7491 (2007).

[17] Q. Nie, X. Li, S. Dai, D. Shin, Z. Chen, X. Gao, *J. Lumin.* **128**, 876 (2008).

[18] B.M. Walsh, N.P. Barnes, D.J. Reichle, S. Jiang, *J. Non-Cryst. Solids* **352**, 5344 (2006).

[19] K. Barczak, T. Pustelny, D. Dorosz, J. Dorosz, *Europ. Phys. J. Spec. Top.* **154**, 11 (2008).

[20] T. Pustelny, J. Ignac-Nowicka, Z. Opilski, *Opt. Appl.* **34**, 563 (2004).

[21] P. Struk, T. Pustelny, K. Gut, K. Gołaszewska, E. Kamińska, M. Ekielski, I. Pasternak, E. Łusakowska, A. Piotrowska, *Acta Phys. Pol. A* **116**, 419 (2009).

[22] I.A.A. Terra, A.S.S. de Camargo, M.C. Terrile, L.A.O. Nunes, *J. Lumin.* **128**, 891 (2008).